Title

Engineered Biosynthesis and Anticancer Studies of Ring-Expanded Antimycin-Type Depsipeptides.

Journal

ACS Synthetic Biology, 13(5)

Authors

Hu, Zhijuan

Gu, Di

Skyrud, Will

et al.

Publication Date

2024-05-17

DOI

10.1021/acssynbio.4c00193

Peer reviewed

HHS Public Access

Author manuscript

ACS Synth Biol. Author manuscript; available in PMC 2024 October 17.

Published in final edited form as:

ACS Synth Biol. 2024 May 17; 13(5): 1562–1571. doi:10.1021/acssynbio.4c00193.

Engineered Biosynthesis and Anticancer Studies of Ring-Expanded Antimycin-Type Depsipeptides

Zhijuan Hu,
Department of Chemical and Biomolecular Engineering, University of California, Berkeley, California 94720, United States; Center of Synthetic Biology and Integrated Bioengineering, School of Engineering, Westlake University, Xihu District, Hangzhou 310024, China

Di Gu,
Department of Chemistry, University of California, Berkeley, California 94720, United States

Will Skyrud,
Department of Chemistry, University of California, Berkeley, California 94720, United States

Yongle Du,
Department of Chemical and Biomolecular Engineering, University of California, Berkeley, California 94720, United States

Rui Zhai,
Department of Chemical and Biomolecular Engineering, University of California, Berkeley, California 94720, United States

Juan Wang,
Department of Chemical and Biomolecular Engineering, University of California, Berkeley, California 94720, United States

Wenjun Zhang
Department of Chemical and Biomolecular Engineering, University of California, Berkeley, California 94720, United States; California Institute for Quantitative Biosciences, University of California, Berkeley, Berkeley, California 94720, United States

Abstract

[*]**Corresponding Authors**: **Zhijuan Hu** – *Department of Chemical and Biomolecular Engineering, University of California, Berkeley, California 94720, United States; Center of Synthetic Biology and Integrated Bioengineering, School of Engineering, Westlake University, Xihu District, Hangzhou 310024, China*; huzhijuan@westlake.edu.cn; **Wenjun Zhang** – *Department of Chemical and Biomolecular Engineering, University of California, Berkeley, California 94720, United States; California Institute for Quantitative Biosciences, University of California, Berkeley, Berkeley, California 94720, United States*; wjzhang@berkeley.edu; Fax: (510) 642-4778.

Author Contributions

W. Z. conceived and supervised the study. Z. H., W. S., D. G., and J. W. designed and performed the experiments. R. Z. carried out the chemical derivatization. Y. D. carried out the structure analysis. W. Z., Z. H., and Y. D. wrote the manuscript.

Supporting Information

The Supporting Information is available free of charge at https://pubs.acs.org/doi/10.1021/acssynbio.4c00193.
Strains, plasmids, and primers used in this study; NMR data of all compounds; ksn gene cluster; metabolites analysis of neoantimycin engineered strains; HRESIMS data of all compounds; NMR spectra of all compounds; bioinformatic analysis of KsnC; protein solubility of PKSs; and MSMS data of compounds **4**, **5**, and **10** (PDF)

The authors declare no competing financial interest.

Respirantins are 18-membered antimycin-type depsipeptides produced by *Streptomyces* sp. and *Kitasatospora* sp. These compounds have shown extraordinary anticancer activities against a panel of cancer cell lines with nanomolar levels of IC_{50} values. However, further investigation has been impeded by the low titers of the natural producers and the challenging chemical synthesis due to their structural complexity. The biosynthetic gene cluster (BGC) of respirantin was previously proposed based on a bioinformatic comparison of the four members of antimycin-type depsipeptides. In this study, we report the first successful reconstitution of respirantin in *Streptomyces albus* using a synthetic BGC. This heterologous system serves as an accessible platform for the production and diversification of respirantins. Through polyketide synthase pathway engineering, biocatalysis, and chemical derivatization, we generated nine respirantin compounds, including six new derivatives. Cytotoxicity screening against human MCF-7 and Hela cancer cell lines revealed a unique biphasic dose–response profile of respirantin. Furthermore, a structure–activity relationship study has elucidated the essential functional groups that contribute to its remarkable cytotoxicity. This work paves the way for respirantin-based anticancer drug discovery and development.

Graphical Abstract

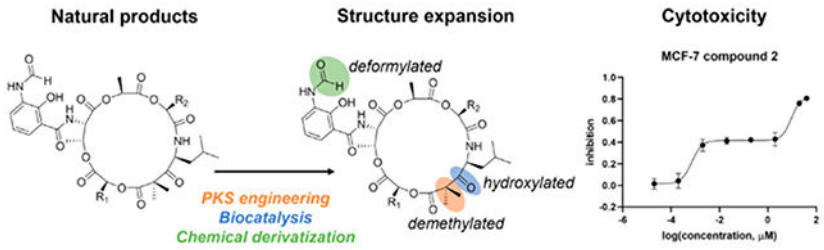

Keywords

biosynthesis; respirantin; PKS engineering; anticancer activity; biphasic dose–response

INTRODUCTION

Natural products, particularly those synthesized by polyketide synthases (PKSs) and nonribosomal peptide synthetases (NRPSs), are noted for their chemical diversity and therapeutic value.[1,2] Antimycin-type depsipeptides are such a family of natural products that possess outstanding anticancer activities.[3] Key members of this family include antimycin, JBIR-06, neoantimycin, and respirantin, which share a common structural skeleton consisting of a macrocyclic ring with an amide linkage to a 3-formamidosalicylate unit and primarily differ in the size of their macrolactone rings (Figure 1).[3,4]

The most well-recognized members of the antimycin-type depsipeptides are the 9-membered antimycins. They are produced by various *Streptomyces* species and so far, more than 40 antimycin analogues by varying the alkyl and acyl chains at C5 and C6 have been reported (Figure 1).[5–10] Extensive studies revealed that antimycins induced cancer cell apoptosis by inhibiting mitochondrial electron transport chain[11–13] and Bcl2/$BclX_L$-related antiapoptotic proteins.[14,15] JBIR-06 and neoantimycins are the 12-membered and

15-membered antimycin-type depsipeptides, respectively (Figure 1). They have also shown promising anticancer activities by down-regulating the expression of GRP-78, a key component of the unfolded protein response and a key determinant in the survival of solid tumors.[16–19] Our recent cellular distribution study of antimycin and neoantimycin inside live cancer cells indicated different subcellular localizations, consistent with the proposed different modes of action of these compounds' varying ring sizes.[20]

The antimycin-type depsipeptide family is further extended by the 18-membered ring class respirantins (Figure 1). Respirantin was initially isolated from a soil *Streptomyces* sp. collected in Japan and revealed to have insecticidal activity.[21] Later, respirantin, along with two analogues, was reisolated from a *Kitasatospora* sp. collected in Alaska.[22] Among the antimycin-type depsipeptide family, the 18-membered respirantins have shown the most potent anticancer activities against a panel of cancer cell lines, including lymphocytic leukemia, pancreas, breast, CNS, colon, lung, and prostate cancer cells with nanomolar levels of IC_{50} values.[22] However, further investigation into their modes of action was severely limited by the low titers of the natural producer (10.8 mg respirantin from 380 L *Kitasatospora* sp. fermentation, yield equivalent to 0.028 mg/L[22]). The outstanding anticancer activities and the poor supply issue have prompted two chemical synthesis attempts. Pettit and co-workers reported the first total synthesis of respirantin[23] in a complicated scheme and Batey and co-worker achieved a convergent manner to complete the total synthesis of respirantin with a yield of 5.9% over 13 linear steps.[24] Despite these attempts, chemical synthesis of respirantin and its analogues for further investigations remained challenging.

Compared to chemical synthesis, engineered biosynthesis provides a feasible solution to access complex natural products and their analogues in a facile manner. The biosynthesis of antimycin-type depsipeptides was proposed to be directed by a hybrid NRPS/PKS pathway that is conserved in the enzymes involved in 3-formamidosalicylate formation. The number of NRPS modules in each of the assembly lines differs, resulting in a variation in the macrolactone ring size (Figure 1).[3,4] While the biosynthetic gene cluster (BGCs) for antimycin, JBIR-06, and neoantimycin and their enzymatic logic have been fully identified, the BGC for respirantin biosynthesis has only been proposed by the Magarvey's group through bioinformatic comparison of the four classes of depsipeptides and remains to be verified.[4] The biosynthetic study of respirantin was further hindered, as none of the known native producers was readily available. Reconstituting the biosynthesis of respirantin in a heterologous host could therefore confirm the proposed BGC for respirantin production. Additionally, it would provide an alternative source for these valuable compounds and enable the generation of new respirantin analogues through biosynthetic engineering or chemical derivatization.

Here we report the first reconstitution of the biosynthesis of respirantin in a heterologous host using a synthetic BGC. We further expanded the structural diversity of respirantin to vary the C7 alkyl chain through PKS engineering. Additionally, the C8 hydroxylated and the C3' deformylated analogues were obtained through enzymatic and chemical derivatization, respectively. The subsequent anticancer screening showed that the dimethyl group, keto group, and formyl group were important to the cytotoxicity of respirantins. We also revealed

a unique biphasic dose–response profile of respirantins, while the underlying dual-mode of action warrants further investigation.

RESULTS AND DISCUSSION

Reconstitute the Biosynthesis of Respirantin in *S. albus*.

The predicted respirantin BGC was synthesized and assembled with essential elements for heterologous expression in *Streptomyces* under its native promoter (Figure S1). The resultant vector, pRES, was then conjugated into *Streptomyces albus* J1074 Δ*antC*, an antimycin native producer strain abolishing antimycin production through the *antC* gene knockout,[25] to yield *S. albus* J1074 Δ*antC*/pRES. We analyzed the organic solvent extracts of the resulting strain and identified three unique peaks (compound **1–3**) that were not present in the negative control (Figure 2). These compounds were then purified from large-scale cultures with yields of 1–2 mg/L, which are about 50 times higher than that of the natural producer *Kitasatospora* sp. By comparing the NMR and HR-MS data with the literature, compounds **1–2** were determined to be the known respirantins[21,22,26] (Tables S2, S3 and S9, Figures S3–S7; NMR spectra of all compounds are listed in Figure S4–S33) while compound **3** was a new analogue. Notably, the NMR spectra showed that the far-right peak was a mixture of compound **1** and an isomer **1***, where the R_1 group is isobutyl in **1** and *sec*-butyl in **1***. Separation of the two isomers failed due to their highly similar physicochemical properties, and thus the following derivatization and bioactivity assays were conducted with the mixture (refer to **1** thereafter). Compound **3** has the molecular formula $C_{35}H_{49}N_3O_{13}$ based on its positive mode high-resolution electrospray ionization mass spectroscopy (HRESIMS), which showed an intense peak at *m/z* 720.3347 $[M + H]^+$, corresponding to $C_{35}H_{50}N_3O_{13}^+$ (calcd 720.3338, Δ 1. Three ppm). The difference of 14 Da between the masses of compounds **3** and **2** suggested that **3** has lost one additional CH_2 unit. Inspection of ^{1}H NMR, homonuclear correlation spectroscopy (COSY), and heteronuclear single quantum coherence (HSQC) spectroscopic data of **3** (Table S4 and Figures S8–S12) in comparison to those of **2** indicated that the isoleucine side-chain of **2** at the R_2 position was replaced by the side-chain of valine in **3**. These results confirmed that the predicted BGC was responsible for producing respirantins. Our heterologous expression strain of *S. albus* J1074 Δ*antC*/pRES thus offered a new source of respirantins with a production efficiency comparable to that of antimycins in *S. albus* J1074.

Generate Alkyl Chain Analogues through PKS Engineering.

Expanding the structural diversity of natural products to improve potency and decrease toxicity is necessary for drug development. With the ability to generate respirantin in *S. albus*, we next sought to use this heterologous system to expand its chemical diversity. Given that the alkyl chain incorporated by the PKS module in antimycins was crucial for the anticancer activity,[14,15] it is worthwhile to generate alkyl chain derivatives with ring-expanded antimycin-type depsipeptides.

As shown in Figure 1, the NRPS-PKS hybrid assembly lines for all antimycin-type depsipeptides have a PKS module, but only the 9-membered antimycin assembly line incorporates alkylmalonyl-CoA while the others were proposed to use the more typical

malonyl-CoA substrate as their extender unit. Recently, Abe's group reported the successful generation of alkyl analogues of the 12-membered JBIR-06 through the AT domain substrate recognition motif swapping in SmlC (LRIAPH) with that from AntD (MPAAAH).[27] Bioinformatic analysis of KsnC revealed a substrate recognition motif (LPTAP^{727}H) similar to that of SmlC (Figure S34). Further structural modeling suggested that P727 might be the critical residue dominating substrate preference of the AT domain (Figure S34). We thus applied three strategies to engineer KsnC in respirantin biosynthesis, including the entire AT domain swapping with AntD (AT_{antD}), AT substrate recognition motif swapping (AT_{MPAAAH}), and substrate recognition motif point mutation (AT_{P727A}), to facilitate a comprehensive understanding of substrate selectivity (Figure 3a).

As a result (Figure 3b), strains harboring pRES-AT_{MPAAAH} and pRES-AT_{P727A} retained the production of respirantins while the strain with pRES-AT_{antD} significantly decreased the production of **1**–**3**. We hypothesized that respirantin production abolishment in AT domain swapping (AT_{antD}) may result from the inactivity of the chimeric PKS enzyme in vivo. This hypothesis was partially supported by the insolubility of this chimeric protein expressed in *E. coli* while the point mutant protein was soluble (Figure S35). Next, we searched for possible alkyl chain derivatives in the engineered strains and identified one new compound (**4**) in the strain of pRES-AT_{MPAAAH}, with an *m/z* value of 776.3970, 28 Da higher than that of compound **1** (Figure 3c). Unlike the 12-membered JBIR-06 analogues, the yield of **4** was too low to allow the purification of enough amounts for NMR analysis. We then proposed the planar structure of compound **4** based on its HRMS and MS/MS data in comparison to **1**, as well as the known substrate preference of AntD (Figure S36).

Considering that the extra MT domain in PKSs may hinder the incorporation of non-native alkylmalonate substrates, we then tried to improve the yield of **4** by deactivating the MT domain via the predicted active-site mutagenesis.[25] The resulting strain harboring pRES-AT_{MPAAAH}-MT_{H1221N} showed a slightly higher yield of **4** (~2-fold). Meanwhile, two new major compounds (**6** and **7**) were produced with yields comparable to those of respirantin. Compounds **6** and **7** were then purified, and their structures were determined to be demethylated **1** and **2** by HR-MS and NMR analysis (Tables S5–S6, Figures S3, S13–S22). The production of **6** and **7** indicated that the *cis*-acting MT domain of KsnC generates the geminal-dimethyl moiety by acting twice upon a malonate unit during the biosynthesis of respirantin. This activity was consistent with the proposed activity of the MT domain of NatC, which was implied by isotope-labeling experiments.[25]

Our AT engineering efforts to generate 18-membered respirantin analogues showed different outcomes compared to the reported 12-membered JBIR-06 analogues; we thus further explored the 15-membered neoantimycin system by testing similar strategies. A soluble NatC chimera was obtained from *E. coli* in which the AT domain of NatC was replaced by that of AntD (NatC-AT_{antD}) (Figure S35). In addition, the MT domain of AntC was inactivated via active-site mutagenesis to yield NatC-AT_{antD}-MT_{H1189N}. The corresponding engineering strains were constructed based on our neoantimycin-producing strain, 5c-1, with modified pCRISPomyces plasmid.[25,28] Metabolomic analysis revealed that similar to the respirantin system, native neoantimycins were produced as the main products in the AT domain swapping strain (Figure S2). An alkylated analogue was also detected (**5**), with the

predicted same alkyl chain as compound **4** (Figures S2 and S37) but only in a trace amount. Further introduction of the MT point mutation led to an ~3-fold increase in the titer of **5** (Figure S2).

The PKS engineering results on producing both 18-membered respirantin analogues and 15-membered neoantimycin analogues suggested that the simplified substrate recognition motif of AT, as well as the entire AT domain, was not sufficient in switching from malonyl-CoA to alkylmalonyl-CoA incorporation in the antimycin-type depsipeptides, particularly for large ring sizes. Different from the 12-membered JBIR-06 assembly line where analogues were efficiently produced via AT engineering alone,[27] both the 15-membered and 18-membered analogues were produced in low efficiency with AT engineering. A possible explanation is that downstream enzymes, including the extra NRPS modules in neoantimycin and respirantin biosynthesis, also play a gatekeeper role, resulting in low titers of alkylated products. While MT disruption seemed to be somewhat helpful in improving the yield of alkylated analogues, additional domain engineering, such as relaxing the possible stringent selectivity of the condensation domain of KsnD and NatD (Figure 1), might be needed to increase the chimeric assembly line efficiency.

Enzymatic and Chemical Derivatization of Respirantin.

In antimycins, the keto group adjacent to the alkyl chain is reduced to a hydroxy group that is further modified by various acyl chains via esterification, which are important for the biological activity of antimycins.[3] Similarly, the keto vs hydroxy group seemed to affect the anticancer activity of neoantimycins toward multiple cancer cell lines.[29] We thus targeted to generate C8 hydroxylated respirantin analogues to assess their anticancer activities. Considering the challenging chemical derivatization due to the labile scaffold of respirantin, we adopted an enzymatic reduction strategy. NatF is the *trans*-acting ketoreductase in neoantimycin biosynthesis, and we proposed that NatF might be capable of reducing the corresponding keto group in respirantin. In vitro biochemical assays with purified NatF, respirantins (**1** or **2**), and nicotinamide adenine dinucleotide phosphate (NADPH) gave rise to new products with expected +2 Da *m/z* values, respectively (Figure 4a), indicating the promiscuous substrate tolerance of NatF. The two reduced respirantins (**8** and **9**) were then purified from large-scale enzymatic reactions, and the successful reduction at the C8 position was confirmed by NMR. In addition, the stereochemistry of C8 was determined as *R* configuration based on NOESY correlations and known absolute configuration of compound **1**, which is consistent with the *R* configuration in neoantimycin (Figure 4b,c, Tables S7, S8, and Figure S3, S23, S33).

One common molecular mechanism of anticancer activity for antimycin-type depsipeptides was the inhibition of oncogenic K-Ras. Antimycin, neoantimycin, and respirantin have all been shown to be potent inhibitors of K-Ras plasma membrane localization with nanomolar IC_{50} values.[30] Structure–activity relationship (SAR) study indicated that the pharmacophore responsible for inhibiting K-Ras PM localization was the 3-formamidosalicylate unit, which was anticipated as this is a conserved unit in all antimycin-type depsipeptides. The *N*-formyl group had been shown to be linked to respiration inhibition of antimycin and anticancer activity of neoantimycin,[20] but its role for the observed potent anticancer activity of

respirantin remained obscure. Through mild acid hydrolysis of compound **1**, we obtained and purified the deformylated respirantin analogue (kitastatin, **10**) for additional anticancer activity screening (Figures 4d and S38).

Cytotoxicity Screening and SAR Analysis of Respirantin.

To investigate the effects of structural variations on cytotoxicity, we obtained the IC_{50} values of compounds **1–3** and **6–10** against the human breast cancer cell line MCF-7 and the human cervical cancer cell line Hela. To our surprise, compounds **1–3** exhibited a biphasic dose–response curve in both cell lines (Figure 5). The percent inhibition increased with increasing concentration of compounds to reach the first plateau around 40%, maintained for several doses, and increased again to reach the second plateau around 80%, giving rise to two IC_{50} values. The IC_{50}-1 values of compounds **1** and **2** were comparable to those from the literature,[22] where the past study might have only screened the low-concentration ranges and missed the second curve. Compounds **6–10** displayed higher IC_{50} values than compounds **1–3** while most of their second IC_{50} values were not determined due to limited compound solubility to reach the second plateau (Figure 5 & Table 1). Notably, anticancer compounds have rarely been reported to have such a biphasic curve. One known case is the tubulin-stabilizing agent docetaxel.[31] Two modes of action were proposed for its biphasic profile: with a concentration of 2–4 nM, cells went through aberrant mitosis followed by necrosis, while with a concentration of 100 nM, cells experienced mitotic arrest followed by apoptosis. The other case are two synthetic anticancer ruthenium-arene Schiff-base complexes, but the mechanism remains to be elucidated.[32]

Our SAR study revealed that compound **2** had the highest cytotoxicity in both cell lines. IC_{50} values of its demethylated analogue **7** and hydroxylated analogue **9** increased 1000-fold and 100-fold, respectively, indicating its sensitivity to the dimethyl group and keto group modifications. In addition, a minor alkyl chain variation at the R2 position also decreased its toxicity by 3—5-fold as observed from compound **3**. The situation was more complicated in compound **1**, which was 2-fold more toxic in Hela cells than in MCF-7 cells. While compound **1** was resistant to dimethyl group depletion in MCF-7 cells, its toxicity decreased 10-fold in its demethylated analogue **6** in Hela cells. IC_{50} values of its hydroxylated analogue **8** increased 10-fold in both cell lines. The deformylated analogue **10** also became less cytotoxic, but its IC_{50} values only increased by 15-fold in MCF-7 and 25-fold in Hela cells, respectively, in contrast to neoantimycin of which the formyl group was critical for its cytotoxicity.[20] Overall, our SAR study suggested that the dimethyl group, keto group, and formyl group were all important for respirantin's outstanding cytotoxicity. Compound **1** seemed to be less active but more resistant to structural variation than compound **2**, despite their subtle structural variation at the R1 position.

CONCLUSIONS

In this study, we confirmed the proposed BGC for respirantin and reconstituted the biosynthesis of respirantin in *S. albus* for the first time. This heterologous system served as a useful platform to obtain and further diversify this class of 18-membered antimycin-type depsipeptides with potent anticancer activity. A total of nine respirantin-like compounds,

six of which are new, were produced via pathway engineering, biocatalysis, and chemical derivatization. SAR study further revealed important functional groups contributing to the outstanding cytotoxicity of respirantin, while the unusual biphasic dose–response profile of respirantin suggested an interesting mode of action for future investigation.

EXPERIMENTAL SECTION

General Experimental Procedures.

Chemicals and media were purchased from Fisher Scientific or Sigma-Aldrich unless otherwise stated. PrimeStar GXL polymerase (Takara) was used for the PCR reactions. Restriction and ligation enzymes were purchased from New England Biolabs unless otherwise stated. Oligonucleotides were purchased from Integrated DNA Technologies (IDT). LC—MS analysis was performed on an Agilent Technologies 6545 Accurate-Mass QTOF LC—MS instrument. The NMR measurement was performed on a Bruker ADVANCE 900 MHz NMR spectrometer equipped with a cryoprobe.

Heterologous Expression.

The respirantin BGC was assembled from synthetic DNA (Thermo Fisher Scientific). The protein-coding portion of the sequence was first codon-juggled to remove BsmBI cut sites and to overcome synthesis constraints. This sequence was subsequently partitioned into 21 synthesizable fragments of 1.9 kb flanked by 60 mer overlapping linkers and BsmBI sites allowing excision from the vendor-provided vectors, using the BOOST software package.[33] After BsmBI digesting and gel purifying the cloned synthetic fragments, PCR fusion was performed to generate 7 intermediate constructs comprising 3 starting fragments each into pENTR, which were transformed to *E. coli* Top10 cells (New England Biolabs), PCR screened for inserts, and sequence verified by the PacBio sequencing platform (Pacific Biosciences). Upon validation, the 7 intermediate fragments were excised by BsmBI and transformed together with pCC1FOSYS, linearized by NotI, into *Streptomyces cerevisiae* CEN.PK2 (Euroscarf, Germany). DNA was purified from resulting colonies and transformed to *E. coli* Top10 where constructs were PCR screened and sequence verified (Pacific Biosciences), then purified for subsequent expression and analysis. The resulting vector (pRES) was mobilized to *S. albus* J1074 Δ*antC* by cross-genera conjugation from *E. coli* WM6026 as previously described.[25] The resultant heterologous expression strains were cultured in 2 mL of tryptic soy broth (TSB) medium for 2 days with shaking at 30 °C. The seed cultures were then inoculated into 30 mL of R5 medium and cultured for 5 days at 30 °C with shaking. The culture broth was extracted with the same volume of EtOAc twice. The EtOAc layers were combined, dried, and resuspended in MeOH. A 100 μL culture equivalent was analyzed by LC—MS. The LC—MS analysis was performed on an Agilent Technologies 6545 Accurate-Mass QTOF LC—MS instrument fitted with an Agilent Eclipse Plus C18 column (4.6 × 100 mm) using a linear gradient of 10—98% CH_3CN (v/v) over 20 min in H_2O with 0.1% formic acid at a flow rate of 0.5 mL/min.

Large-Scale Fermentation and Isolation.

The heterologous expression strain was inoculated in TSB medium for 2 days as seed and further cultured in 30 L of R5 medium (30 mL per flask) for 5 days at 30 °C with shaking.

The culture broth was extracted with EtOAc twice. The crude extract was subjected to silica gel column chromatography and eluted with 50% hexane-ethyl acetate. The fractions containing respirantins were combined and further purified by semipreparative HPLC with a Phenomenex Luna C18 column (5 μm, 250 × 10 mm) using an isocratic condition of 90% CH_3CN (v/v) in H_2O with 0.1% formic acid at a flow rate of 3.5 mL/min. Structure determination is included in Supporting Information.

Respirantin PKS Engineering.

Spectinomycin resistance gene (*smR*) was amplified from pIJ778 with primers (RED-smR-f and RED-smR-r) and inserted into pRES before *ksnC* by PCR targeting with pKD46.[34] The resultant plasmid pRES-smR was transformed to WM6026 and then conjugated into *S. albus* J1074 Δ*antC*. *ksnC* mutant plasmids were constructed by two-step PCR targeting. The first step is to replace the KS-AT didomain of *ksnC* with a tetracycline resistance gene (*tet*). *Tet* was amplified with primers (RED-tet-f and RED-tet-r/RED-MT-tet-r) and used to replace KS-AT by PCR targeting with pKD46. The resultant plasmid pRES-tet or pRES-MT-tet (KS-AT-MT tridomain replaced with tet) was used for the second PCR-targeting. KS-AT was amplified from pRES into two fragments with P727A mutation using primers (KS-f and AT-P727A-r, AT-P727A-f and RED-r) and assembled by PCR. smR fragment was amplified using primers (RED-smR-f and RED-smR-r) and ligated with KS-AT(P727A) by PCR to afford smR-AT(P727A). Fragment smR-AT(antD) was generated similar to that above, using primers (KS-f and KS-r for KS from ksnC, AT-f and RED-AT-r for AT from antD). Fragment smR-AT(MPAAAH) was generated based on smR-KS-AT(P727A) using primers (RED-smR-f and MPAAAH-r, MPAAAH-f and RED-r). Fragment smR-AT(MPAAAH)-MT(H1221N) was generated using pRES-smR-KS-AT-(MPAAAH) as a template with primers (RED-smR-f and RED-MT-r). Fragments smR-AT(P727A), smR-AT(antD), smR-AT(MPAAAH), and smR-AT(MPAAAH)-MT-(H1221N) were used to do the second PCR targeting to generate plasmids pRES-smR-AT(P727A), pRES-smR-AT-(antD), pRES-smR-AT(MPAAAH), and pRES-smR-AT-(MPAAAH)-MT(H1221N), respectively, by PCR targeting with pRES-tet or pRES-MT-tet and pKD46. These plasmids were transformed to WM6026 and then conjugated into *S. albus* J1074 Δ*antC*.

NatF In Vitro Assay.

Overexpression and purification of NatF were the same as before.[25] The purified protein (10 μM) was incubated with 200 μM substrate in 500 μL of buffer containing 2 mM NADPH and 50 mM Tris-HCl (pH 8.0). Ten reactions were set up and incubated at 30 °C overnight and quenched by extraction with ice-cold EtOAc twice. The EtOAc layers were combined, dried under a nitrogen concentrator, and further purified by semipreparative HPLC with a Phenomenex Luna C18 column (5 μm, 250 × 10 mm) using an isocratic condition of 90% CH_3CN (v/v) in H_2O with 0.1% formic acid at a flow rate of 3.5 mL/min.

Acidic Hydrolysis of Compound 1.

Compound **1** was incubated with 4 equiv of Urea HCl in a 1:1 ratio of water/EtOH mixed solution at 55 °C overnight. The deformylated product was purified by semipreparative

HPLC with a Phenomenex Luna C18 column (5 μm, 250 × 10 mm) using an isocratic condition of 85% CH_3CN (v/v) in H_2O at a flow rate of 3.5 mL/min.

Cytotoxicity Assay.

The cytotoxicity of the isolated compounds against MCF-7 and Hela cells was evaluated using Cyto Scan SRB cell cytotoxicity assay kit according to manufacturer's instructions. Briefly, cells were seeded in 96-well plates at 5000 cells/well confluence and incubated at 37 °C with 5% CO_2 for 24 h, followed by treatment with test compounds at appropriate concentrations. After further 72 h incubation for MCF-7 cells (48 h for Hela cells), 50 μL of a fixative reagent was gently layered onto each well. The plate was incubated at 4 °C for 1 h, washed 4 times with distilled water, and dried in a 50 °C incubator for 30 min. Then, 100 μL of SRB dye solution was added and incubated for 30 min at room temperature in the dark. The wash and dry step were repeated with a wash solution instead of water. The dye was dissolved with 200 μL of SRB solubilization buffer and absorbance was measured at 515 nm. DMSO was used as a negative control. Absorbances were blanked with cell-free medium controls. Percent inhibition = (cell control – experimental)/cell control. IC_{50} values were calculated using GraphPad Prism 9.

Supplementary Material

Refer to Web version on PubMed Central for supplementary material.

ACKNOWLEDGMENTS

We thank the DNA Synthesis Science Program of DOE Joint Genome Institute (JGI) for synthesizing the entire respirantin BGC for heterologous expression. This research was also financially supported by the grant to W.Z. from the American Cancer Society. We thank the Berkeley Cell Culture Facility for providing cell culturing services for the cytotoxicity assays.

REFERENCES

(1). Süssmuth RD; Mainz A Nonribosomal Peptide Synthesis-Principles and Prospects. Angew. Chem., Int. Ed 2017, 56 (14), 3770–3821.

(2). Nivina A; Yuet KP; Hsu J; Khosla C Evolution and Diversity of Assembly-Line Polyketide Synthases. Chem. Rev 2019, 119 (24), 12524–12547.

(3). Liu J; Zhu X; Kim SJ; Zhang W Antimycin-Type Depsipeptides: Discovery, Biosynthesis, Chemical Synthesis, and Bioactivities. Nat. Prod. Rep 2016, 33 (10), 1146–1165.

(4). Vanner SA; Li X; Zvanych R; Torchia J; Sang J; Andrews DW; Magarvey NA Chemical and Biosynthetic Evolution of the Antimycin-Type Depsipeptides. Mol. BioSyst 2013, 9 (11), 2712–2719.

(5). Dunshee BR; Leben C; Keitt GW; Strong FM The Isolation and Properties of Antimycin A. J. Am. Chem. Soc 1949, 71 (7), 2436–2437.

(6). Shiomi K; Hatae K; Hatano H; Matsumoto A; Takahashi Y; Jiang CL; Tomoda H; Kobayashi S; Tanaka H; Omura S A New Antibiotic, Antimycin A9, Produced by Streptomyces Sp. K01–0031. J. Antibiot 2005, 58 (1), 74–78.

(7). Hosotani N; Kumagai K; Nakagawa H; Shimatani T; Saji I Antimycins A10-A16, Seven New Antimycin Antibiotics Produced by Streptomyces Spp. SPA-10191 and SPA-8893. J. Antibiot 2005, 58 (7), 460–467.

(8). Yan LL; Han NN; Zhang YQ; Yu LY; Chen J; Wei YZ; Li QP; Tao L; Zheng GH; Yang SE; et al. Antimycin A 18 Produced by an Endophytic Streptomyces Albidoflavus Isolated from a Mangrove Plant. J. Antibiot 2010, 63 (5), 259–261.

(9). Han Z; Xu Y; McConnell O; Liu L; Li Y; Qi S; Huang X; Qian P Two Antimycin A Analogues from Marine-Derived Actinomycete Streptomyces Lusitanus. Mar. Drugs 2012, 10 (12), 668–676.

(10). Yan Y; Chen J; Zhang L; Zheng Q; Han Y; Zhang H; Zhang D; Awakawa T; Abe I; Liu W Multiplexing of Combinatorial Chemistry in Antimycin Biosynthesis: Expansion of Molecular Diversity and Utility. Angew. Chem., Int. Ed 2013, 52 (47), 12308–12312.

(11). Pham NA; Robinson BH; Hedley DW Simultaneous Detection of Mitochondrial Respiratory Chain Activity and Reactive Oxygen in Digitonin-Permeabilized Cells Using Flow Cytometry. Cytometry 2000, 41 (4), 245–251.

(12). King MA; Radicchi-Mastroianni MA Antimycin A-Induced Apoptosis of HL-60 Cells. Cytometry 2002, 49 (3), 106–112.

(13). Labs M; Rühle T; Leister D The Antimycin A-Sensitive Pathway of Cyclic Electron Flow: From 1963 to 2015. Photosynth. Res 2016, 129 (3), 231–238.

(14). Tzung SP; Kim KM; Basañez G; Giedt CD; Simon J; Zimmerberg J; Zhang KYJ; Hockenbery DM Antimycin A Mimics a Cell-Death-Inducing Bcl-2 Homology Domain 3. Nat. Cell Biol 2001, 3 (2), 183–191.

(15). Schwartz PS; Manion MK; Emerson CB; Fry JS; Schulz CM; Sweet IR; Hockenbery DM 2-Methoxy Antimycin Reveals a Unique Mechanism for Bcl-XL Inhibition. Mol. Cancer Ther 2007, 6 (7), 2073–2080.

(16). Umeda Y; Chijiwa S; Furihata K; Furihata K; Sakuda S; Nagasawa H; Watanabe H; Shin-ya K Prunustatin A, a Novel GRP78 Molecular Chaperone Down- Regulator Isolated from Streptomyces Violaceoniger. J. Antibiot 2005, 58 (3), 206–209.

(17). Izumikawa M; Ueda JY; Chijiwa S; Takagi M; Shin-Ya K Novel GRP78 Molecular Chaperone Expression Down-Regulators JBIR-04 and –05 Isolated from Streptomyces Violaceoniger. J. Antibiot 2007, 60 (10), 640–644.

(18). Ueda J; Nagai A; Izumikawa M; Chijiwa S; Takagi M; Shin-ya K A Novel Antimycin-like Compound, JBIR-06, from Streptomyces Sp. ML55. J. Antibiot 2008, 61 (4), 241–244.

(19). Kozone I; Ueda JY; Takagi M; Shin-Ya K JBIR-52, a New Antimycin-like Compound, from Streptomyces Sp. ML55. J. Antibiot 2009, 62 (10), 593–595.

(20). Seidel J; Miao Y; Porterfield W; Cai W; Zhu X; Kim SJ; Hu F; Bhattarai-Kline S; Min W; Zhang W Structure-Activity-Distribution Relationship Study of Anti-Cancer Antimycin-Type Depsipeptides. Chem. Commun 2019, 55 (63), 9379–9382.

(21). Urushibata I; Isogai A; Matsumoto S; Suzuke A Respirantin, A Novel Insecticidal Cyclodepsipeptide from Streptomyces. J. Antibiot 1993, 46 (4), 701–703.

(22). Pettit GR; Tan R; Pettit RK; Smith TH; Feng S; Doubek DL; Richert L; Hamblin J; Weber C; Chapuis J Antineoplastic Agents. 560. Isolation and Structure of Kitastatin 1 from an Alaskan Kitasatospora Sp. J. Nat. Prod 2007, 70 (7), 1069–1072.

(23). Pettit GR; Smith TH; Feng S; Knight JC; Tan R; Pettit RK; Hinrichs PA Antineoplastic Agents. 561. Total Synthesis of Respirantin[1a]. J. Nat. Prod 2007, 70 (7), 1073–1083.

(24). Beveridge RE; Batey RA An Organotrifluoroborate-Based Convergent Total Synthesis of the Potent Cancer Cell Growth Inhibitory Depsipeptides Kitastatin and Respirantin. Org. Lett 2014, 16 (9), 2322–2325.

(25). Skyrud W; Liu J; Thankachan D; Cabrera M; Seipke RF; Zhang W Biosynthesis of the 15-Membered Ring Depsipeptide Neoantimycin. ACS Chem. Biol 2018, 13 (5), 1398–1406.

(26). Akinori S; Kozo N Physiologically Active Substance TOD-4403s, its Use and Production Thereof, 1993.

(27). Awakawa T; Fujioka T; Zhang L; Hoshino S; Hu Z; Hashimoto J; Kozone I; Ikeda H; Shin-Ya K; Liu W; et al. Reprogramming of the Antimycin NRPS-PKS Assembly Lines Inspired by Gene Evolution. Nat. Commun 2018, 9 (1), 3534.

(28). Cobb RE; Wang Y; Zhao H High-Efficiency Multiplex Genome Editing of Streptomyces Species Using an Engineered CRISPR/Cas System. ACS Synth. Biol 2015, 4 (6), 723–728.

(29). Zhou Y; Lin X; Williams SR; Liu L; Shen Y; Wang SP; Sun F; Xu S; Deng H; Leadlay PF; et al. Directed Accumulation of Anticancer Depsipeptides by Characterization of Neoantimycins Biosynthetic Pathway and an NADPH-Dependent Reductase. ACS Chem. Biol 2018, 13 (8), 2153–2160.

(30). Salim AA; Cho KJ; Tan L; Quezada M; Lacey E; Hancock JF; Capon RJ Rare Streptomyces N-Formyl Amino-Salicylamides Inhibit Oncogenic K-Ras. Org. Lett 2014, 16 (19), 5036–5039.

(31). Hernández-Vargas H; Palacios J; Moreno-Bueno G Molecular Profiling of Docetaxel Cytotoxicity in Breast Cancer Cells: Uncoupling of Aberrant Mitosis and Apoptosis. Oncogene 2007, 26 (20), 2902–2913.

(32). Chow MJ; Babak MV; Wong DYQ; Pastorin G; Gaiddon C; Ang WH Structural Determinants of P53-Independence in Anticancer Ruthenium-Arene Schiff-Base Complexes. Mol. Pharmaceutics 2016, 13 (7), 2543–2554.

(33). Oberortner E; Cheng JF; Hillson NJ; Deutsch S Streamlining the Design-to-Build Transition with Build-Optimization Software Tools. ACS Synth. Biol 2017, 6 (3), 485–496.

(34). Gust B; Kieser T; Chater K PCR Targeting System in Streptomyces Coelicolor A3(2); John Innes Centre, 2002; pp 1–39.

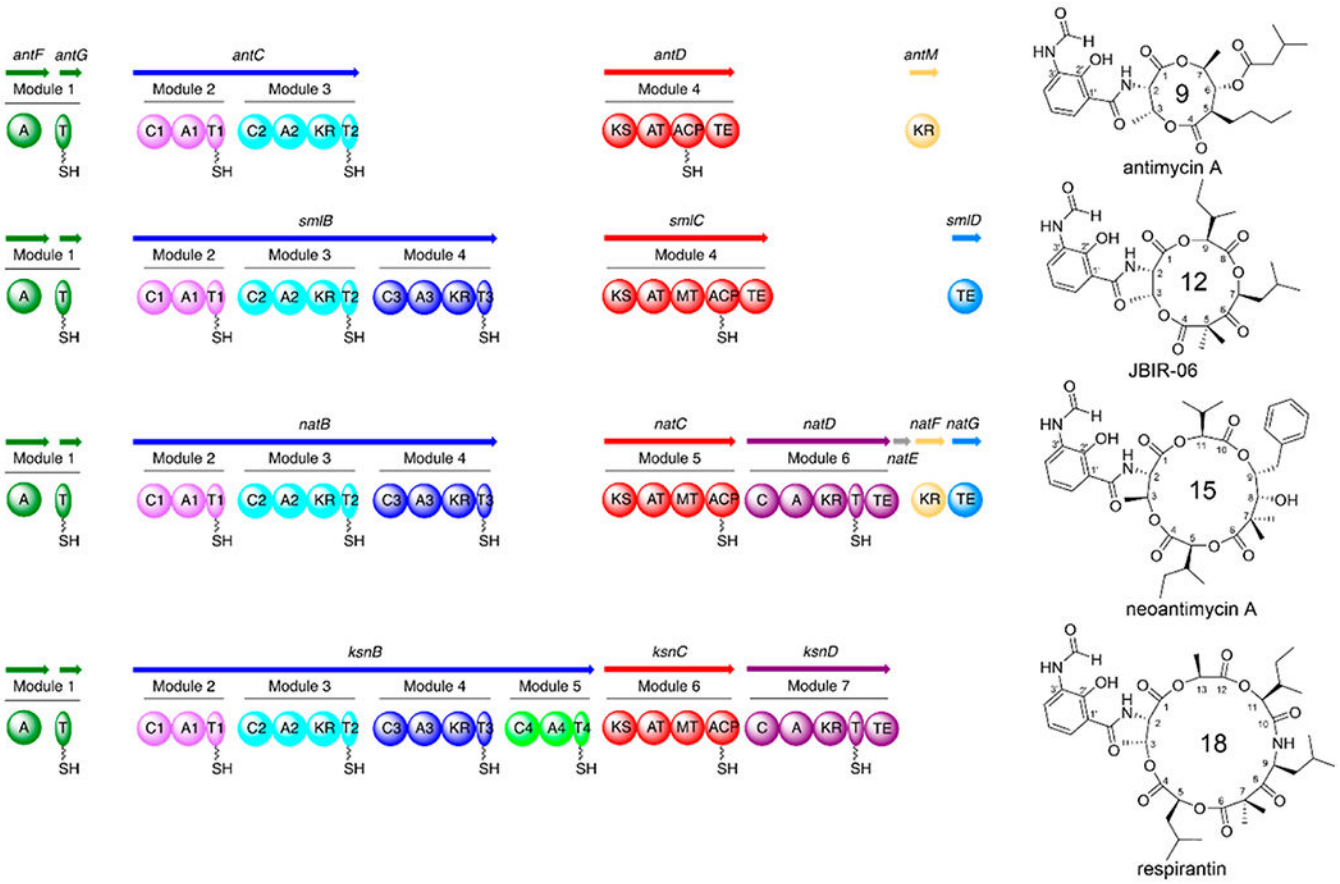

Figure 1.
NRPS-PKS BGCs that are responsible for the four classes of antimycin-type depsipeptide assembly.

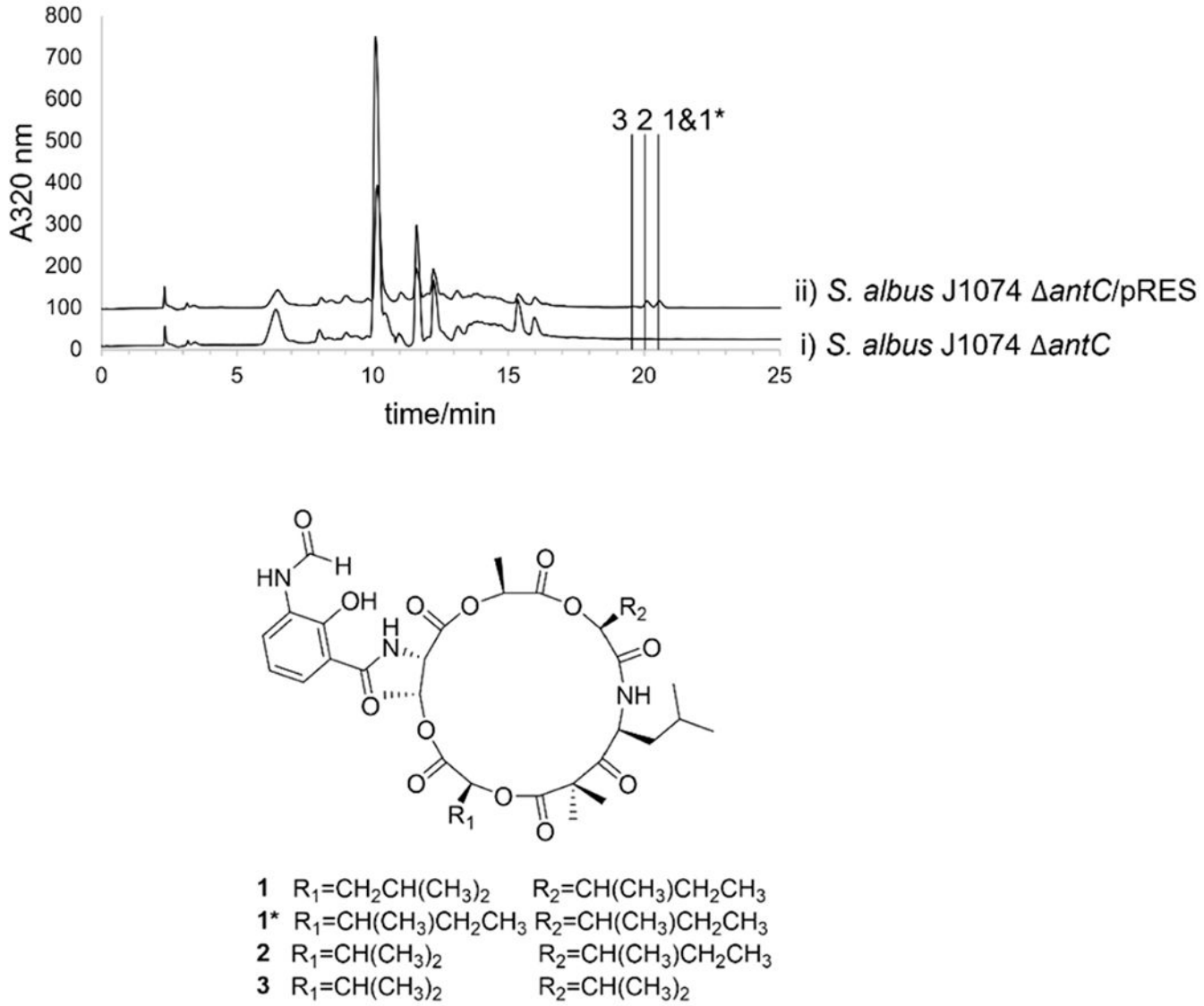

1 $R_1=CH_2CH(CH_3)_2$ $R_2=CH(CH_3)CH_2CH_3$
1* $R_1=CH(CH_3)CH_2CH_3$ $R_2=CH(CH_3)CH_2CH_3$
2 $R_1=CH(CH_3)_2$ $R_2=CH(CH_3)CH_2CH_3$
3 $R_1=CH(CH_3)_2$ $R_2=CH(CH_3)_2$

Figure 2.
Heterologous production of respirantins. UV traces at 320 nm of the EtOAc extracts from (i) *S. albus* J1074 Δ*antC* and (ii) *S. albus* J1074 Δ*antC*/pRES.

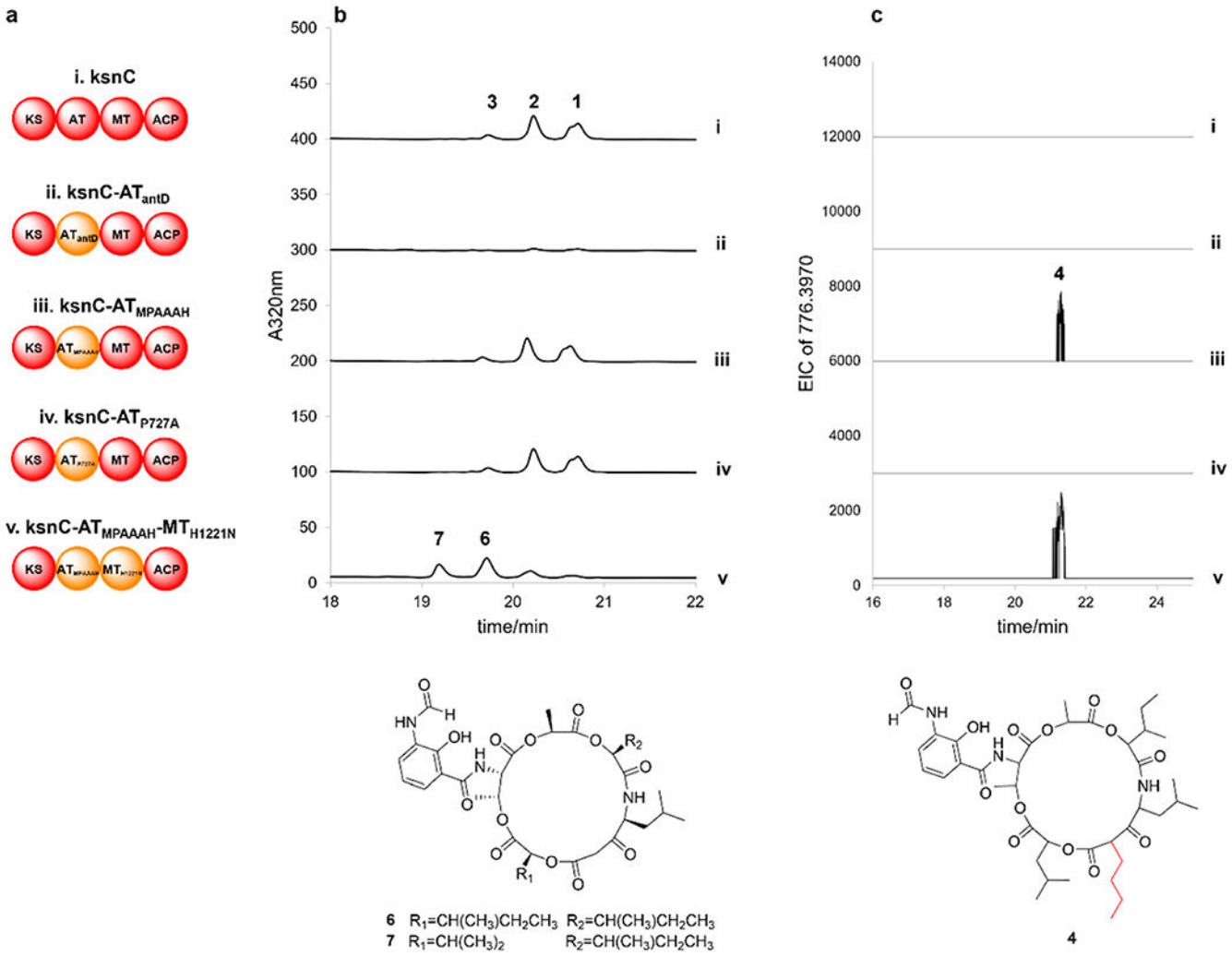

Figure 3.

Metabolites analysis of respirantin PKS engineered strains. (a) Cartoon schematic diagram of engineered *ksnC*. (b) UV traces of respirantin compound **1–3** and desmethyl-respirantin compounds **6–7** at 320 nm from PKS engineered strains. (c) EIC of *m/z* 776.3970 corresponds to alkylated compound **4**.

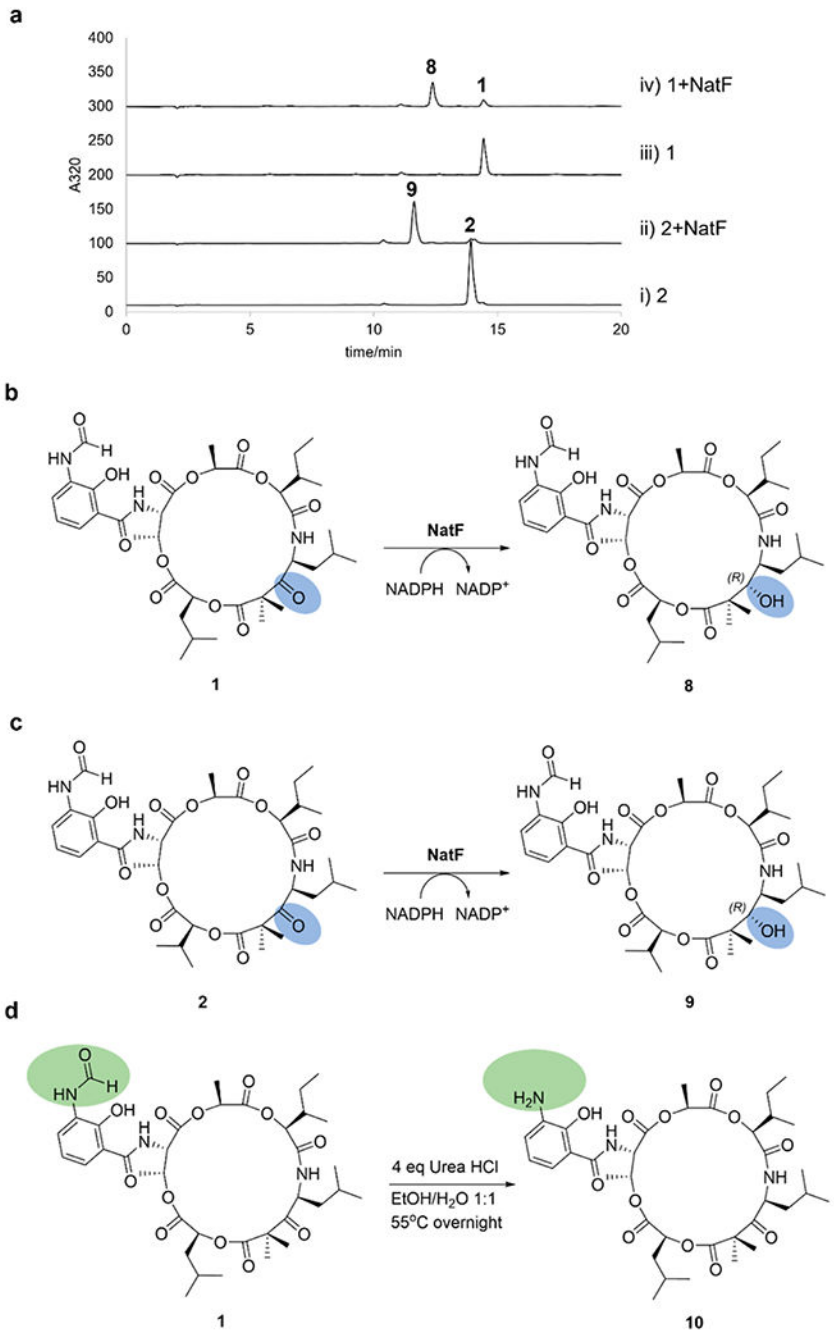

Figure 4.

Enzymatic and chemical derivatization of respirantins. (a) UV traces (320 nm) of NatF in in vitro assays with respirantin compounds **1** and **2.** (b) Scheme of NatF reduction with compound **1.** (c) Scheme of NatF reduction with compound **2.** (d) Scheme of acidic hydrolysis of compound **1.**

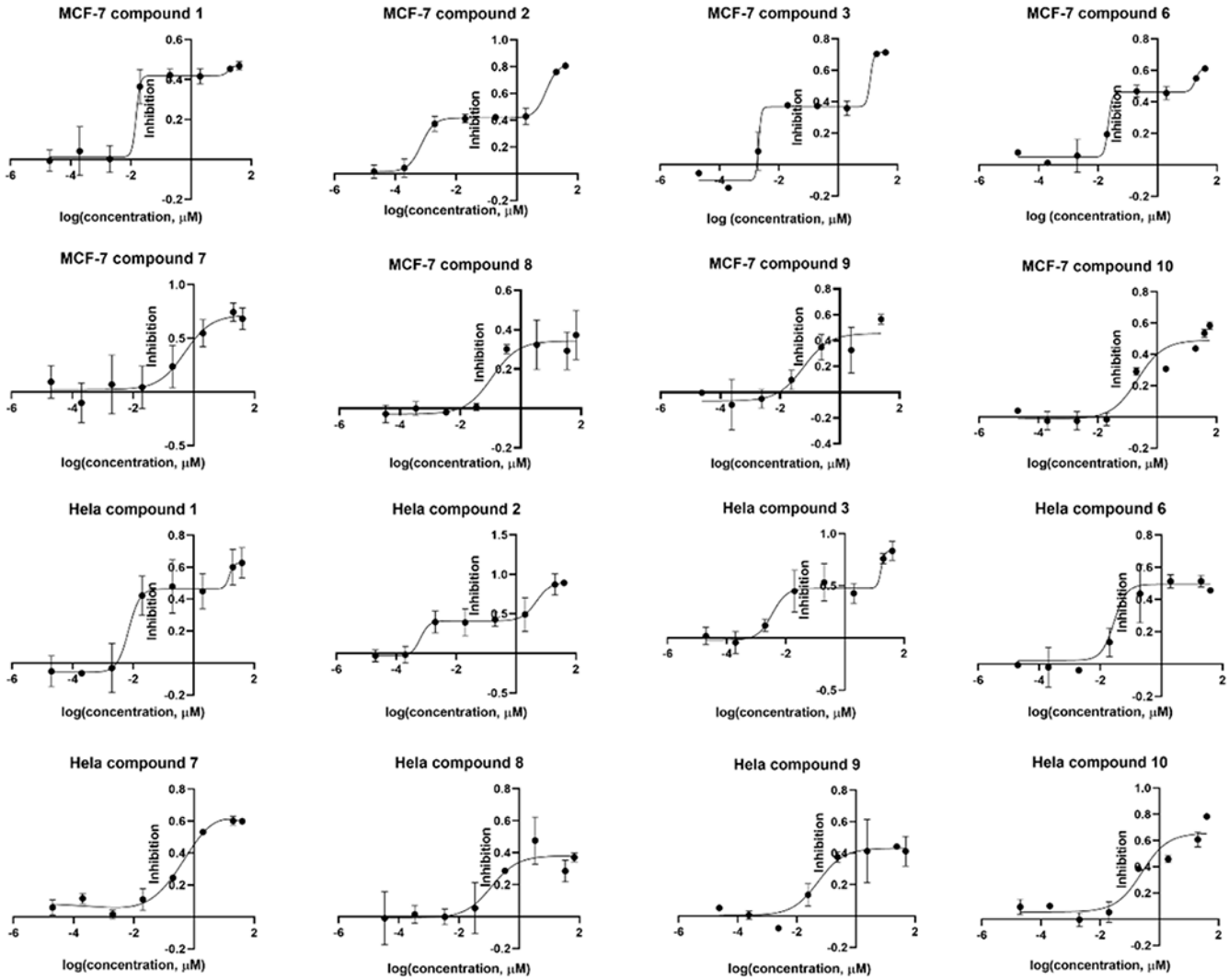

Figure 5.
Dose–response curves of tested compounds against MCF-7 and Hela cells.

Table 1.

IC_{50} Values of Tested Compounds against MCF-7 and Hela Cells[a]

	μM	**1**	**2**	**3**	**6**	**7**	**8**	**9**	**10**
MCF-7	IC_{50}-1	0.0150	0.000716	0.00209	0.0220	0.508	0.112	0.0606	0.220
	IC_{50}-2	17.4	9.27	12.1	18.9	n.d.	n.d.	n.d.	n.d.
Hela	IC_{50}-1	0.00706	0.000632	0.00347	0.0409	0.386	0.0623	0.0523	0.182
	IC_{50}-2	15.2	4.80	16.6	n.d.	n.d.	n.d.	n.d.	n.d.

[a] n.d. means not determined.